

Topological Cluster State Computation with Photons.

Simon J. Devitt,^{1,*} Austin G. Fowler,² Ashley M. Stephens,³ Andrew D. Greentree,³ Lloyd C.L. Hollenberg,³ William J. Munro,^{4,1} and Kae Nemoto¹

¹*National Institute for Informatics, 2-1-2 Hitosubashi, Chiyoda-ku, Tokyo 101-8340, Japan.*

²*Institute for Quantum Computing, University of Waterloo, Waterloo, Canada.*

³*Centre for Quantum Computing Technology, Department of Physics, University of Melbourne, Victoria, Australia*

⁴*Hewlett-Packard Laboratories, Filton Road, Stoke Gifford, Bristol BS34 8QZ, United Kingdom*

(Dated: March 9, 2022)

Entanglement is one of the most mysterious and fleeting properties of nature. It is also a powerful resource for quantum information processing. Efforts to design and build a quantum computer are severely constrained by the difficulties of preserving useful qubit entanglement against the environment. Concatenated fault-tolerant error correction provides a framework to perform scalable computation, but is extremely expensive in terms of resources. Direct topological implementations promise robust entanglement and control, but require physical systems with as yet unobserved controllable topological phases. Here we present the first practical scheme for constructing a topological quantum computer based on a 3D cluster state lattice of photons on chip. In contrast to the resource requirements of other schemes, a target error rate of 10^{-16} requires approximately 10^3 components per logical qubit. This constitutes a significant advance towards practical quantum computing and leads the way for topological architectures in other implementations.

The recent introduction by Raussendorf, Harrington and Goyal of Topological cluster State computing [1, 2, 3, 4] marks an enormous milestone in the advance of theoretical techniques for quantum information processing (QIP). This model of QIP differs significantly from both the circuit model of computation and more traditional cluster state computing [5] in that the entanglement resource defines a topological “backdrop” where information qubits can be defined in a very non-local ways. The disconnect between the physical qubits (used to construct the lattice) and information qubits (non-local correlations within the lattice) allows information to be topologically protected and consequently is inherently robust against local perturbations caused by quantum errors occurring on the physical system. This exploitation of topological protection utilizing qubits, rather than more exotic anyonic quantum systems, which are difficult to experimentally create and manipulate [6], leads to an extraordinary computational model that exhibits high fault-tolerant thresholds, naturally corrects problematic error channels such as qubit loss and does not require exorbitant resource costs for a high level of error correction.

The scientific effort to construct a large scale device capable of QIP has advanced significantly over the past decade. Many experimental systems such as ion traps, superconductors, single photonics, hybrid atom/molecular/optical systems and charge/donor based quantum devices have shown remarkable experimental progress with each demonstrating the basic ingredients necessary for QIP [7, 8, 9, 10, 11, 12, 13, 14, 15, 16]. However, there is currently no experimental or theoretical work attempting to adapt any of these physical QIP systems to the topological cluster model. Matter based qubit systems generally not appropriate to realize full 3D topological cluster states. As the total length of a 3D cluster computation is related to one of the lattice dimensions, longer computations would require more and more physical qubits which must be physically entangled in complicated ways, a difficult prospect for a physical device. Surface code computation [2, 3], which is closely related to 3D topological clusters, is instead utilized, but as yet, no detailed quantum architecture has been proposed to implement this modified model.

In contrast, photonic qubits are an ideal candidate to realize topological cluster state QIP. Photons are highly mobile objects and are essentially free, provided an appropriate single photon source is available. Therefore, if an optical entanglement network can be constructed, photons can be continually injected from on demand sources, creating the required 3D cluster state. Linear optical quantum computation [17, 18] which is based on single photons as the qubits, linear optical elements such as beamsplitters, optical wave plates and single photon detectors is one of the most successful experimental systems with many fundamental gates and algorithms demonstrated [16, 18]. In current experimental setups, there are real fundamental problems towards large-scale QIP both theoretically and experimentally. For instance, the development of an experimentally feasible truly large scale architecture for photons is hampered by the fact that measurement induced photon/photon interactions are intrinsically probabilistic [18], necessitating non-trivial photon routing and storage for large scale architectures.

*Electronic address: devitt@nii.ac.jp

The cluster state model of quantum computation [5] was one of the first major breakthroughs in optical QIP, mitigating the issue of probabilistic gate operations [19] by translating the problem of high failure rates in gate operations to a problem of probabilistically growing large clusters, off-line, to be consumed for quantum computation. Theoretically the cluster state model can be the ideal solution to the optics probabilistic gates, however, it exhibit serious problems in its realization. One significant hurdle is photon loss. As qubit information in cluster state computation is, at each time step, physical located on individual qubits, photonic loss results in the loss of algorithmic information. Consequentially, cluster states need to incorporate photon non-demolition detection (which can be incorporated into the probabilistic entangling gates [20]) or dedicated loss correction codes [21, 22] that need to be incorporated in addition to protecting against standard quantum errors. A secondary issue is traditional error correction for clusters, which is heavily based on traditional coding schemes [23] and hence suffer from arguably unrealistic thresholds and significant computational overhead [24, 25, 26]. Although the cluster state approach in optics has technological problems, it certainly pushed optical QIP to the level of other matured implementations such as ion trap experiments.

Probabilistic growth techniques for creating a 3D cluster for topological computing is a major problem as the topological protection afforded to quantum information is predicated on a large lattice existing before qubits are defined. Hence if there is any hope for a realistic physical implementation of this model a deterministic optical entangling operation is required. Such operations could for instance include the C-Phase and parity gates [27, 28, 31], and may be via a direct photon-photon interactions, cavity QED techniques [29, 30] or an indirect bus mediated quantum nondemolition like interaction [31, 32]. We are going to focus on the later with the recently introduced idea of the photonic module and chip [32, 33]. This small scale, chip based quantum device is an illustrative example of a technology with all the essential components to create the required cluster lattice for the 3D topological model. This device has the flexibility to entangle an arbitrary number of photons with no dynamical change in its operation and the manner in which photons flow in and out of the unit make it an ideal component to realize topological cluster state computing.

This paper introduces how the photonic chip can be utilized to realize this model of computation. This 3D preparation network continuously prepares the lattice, face by face, quickly, deterministically with small operational elements which can be fabricated on-chip. This leads to an experimentally feasible optical computer architecture, based on independently manufactured photonic chips which can implement arguably the most advanced computational scheme devised to date, exhibiting high thresholds at comparatively low resource costs. The benefits of adapting topological cluster state computing to single photons with the photonic chip cannot be overstated, for example,

- The optical network prepares the lattice continuously and deterministically with no need for photonic storage. Each lattice face can be measured immediately as part of the computation after exiting the preparation network. As storage is not required, it is expected that photon loss rates will consequently decrease and the required error protection (and hence physical resources) for a large quantum algorithm will be reduced.
- Photon loss does not lead to catastrophic loss of information when computing topologically, since the physical qubits do not encode the algorithmic information: algorithmic qubits are instead defined via defects in this lattice, not by individual photons.
- Topological cluster state computation has one of the highest thresholds of any model of quantum computation. While adaptations of post-selected schemes [34] have, to an extent, reduced the prohibitively high resource costs to a more experimentally feasible level, the application of such schemes to an underlying physical system (specifically in optics) has yet to be fully developed.
- More traditional techniques for concatenated quantum error correction roughly allow for a double exponential suppression in logical error rates for an exponential increase in resources. In contrast, topological cluster states allow for an exponential suppression in logical error rates with a linear increase in resources. While both scalings lead to an exponential improvement, the linear scaling of topological coding allows for much more flexibility in tailoring error correction to the physical error rates without exponential fluctuations of physical resources.
- The network is a continuous generator of the cluster. The 2D cross section of the lattice, which defines the total number of qubits and/or topological protection available to the computer, is the only determining factor in the number of photonic modules/chips required. Additionally, as the optical preparation network is constructed from reasonably simple operational elements (the photonic chip and photonic module), each chip can be fabricated and characterized independently giving us a computational architecture which scales in a very straightforward manner. Additional chips are simply linked to the preparation network as they become available, arbitrarily increasing the 2D cross section of the lattice and consequently increasing the size and/or topological protection of the computer.

- The ability to fabricate photonic chips leads to a static network. The routing and switching pattern for the preparation of the 3D lattice does not change depending on the size of the lattice or the number of time steps required for computation. This is a significant advantage over traditional optical architectures which require dynamical routing based on the success/failure of individual probabilistic gates [19] and is even a benefit over more advanced percolation techniques [35] which largely eliminate the need for dynamical routing but does not address the issue of storage.
- The resource requirements for this architecture is extremely promising. We will show that the network required to perform large scale optical computing using 3D clusters requires a number of chips which grows linearly with the cross sectional size of the lattice. Basic estimates will show that performing a large scale computation with $\approx 10^{16}$ logical operations only requires approximately 3000 fabricated devices per logical qubit.

The following discussions will illustrate the lattice preparation network, utilizing the photonic chip illustrated in Fig. 1 as the basic building block of the computer. We will detail the physical layout of the network, the optical switching sequence required and several techniques that are used to optimize the preparation of the cluster. We complete the discussion with a resource analysis, examining the number of fabricated devices required to perform a large scale quantum algorithm.

Fig 2 illustrates the general physical structure of the architecture. Fig 2a. shows the general layout of the computer where only one (of four) stages of the preparation network is illustrated for clarity. Initially unentangled photons enter the preparation network from the rear, flow through a static network of photonic chips and exit the preparation network where they can be immediately consumed for computation. Fig 2b. illustrates a single unit cell of the cluster state which repeats and extends in all three dimensions. Computation proceeds by consuming successive faces (we define successive faces as running from right to left in Fig 2b. and for the remainder of this paper), which acts to simulate time through the computation. Note that the cluster is not a fully connected 3D lattice. Each photon is only connected to four neighbors (not six). This implies that there are two sets of optical lines, one set runs at a fixed repetition rate (the red photons in Fig 2b.) which we denote as full rate lines. The other half run at half that rate (black photons) and are denoted half rate lines. If you examine the cluster from the front or rear, the full and half rate lines form a checkerboard pattern.

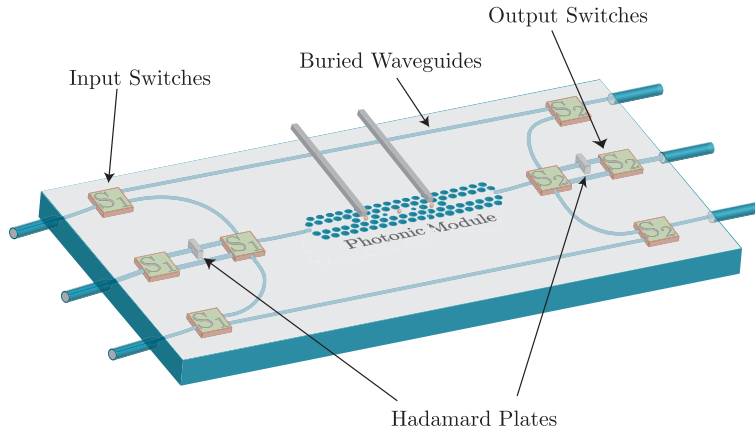


FIG. 1: **Schematic design for the photonic chip.** The chip is a 3-in 3-out integrated device containing one photonic module [32] and classical single photon routing. Not shown are Hadamard plates required on each input/output port. The single photon routing for the chip requires each port to be switched to the module or a bypass line with the option of routing a photon in the upper (or lower) port through the bypass at the same time as a photon is sent into the module on the central line (with the option of applying a Hadamard rotation before and after the interaction with the module).

The total 2D size of a single slice of the cluster dictates the total number of algorithmic qubits available and/or and the topological protection the computer has. Each qubit in the lattice is linked to four others, and the total state of the lattice can be specified via stabilizers [36]. The lattice is a unique state which is a simultaneous $+1$ eigenstate of the operators $ZZX^{i,j}ZZ$, where Z and X are the 2×2 Pauli operators, (i, j) are the co-ordinates of each of the N photons in the 3D lattice, the Z operators applied to qubits linked to the node qubit (i, j) and the $N - 5$ identity operators are implied. For photons that do not have four nearest neighbors (i.e. at edges of the lattice), the associated stabilizer retains of this form but excludes the operator(s) associated with the missing neighbor(s).

The optical network required to prepare such a state requires the forcible projection of a group of photons into these required eigenstates. Fig 1 illustrates the construction of the photonic chip [33] which is utilized to perform

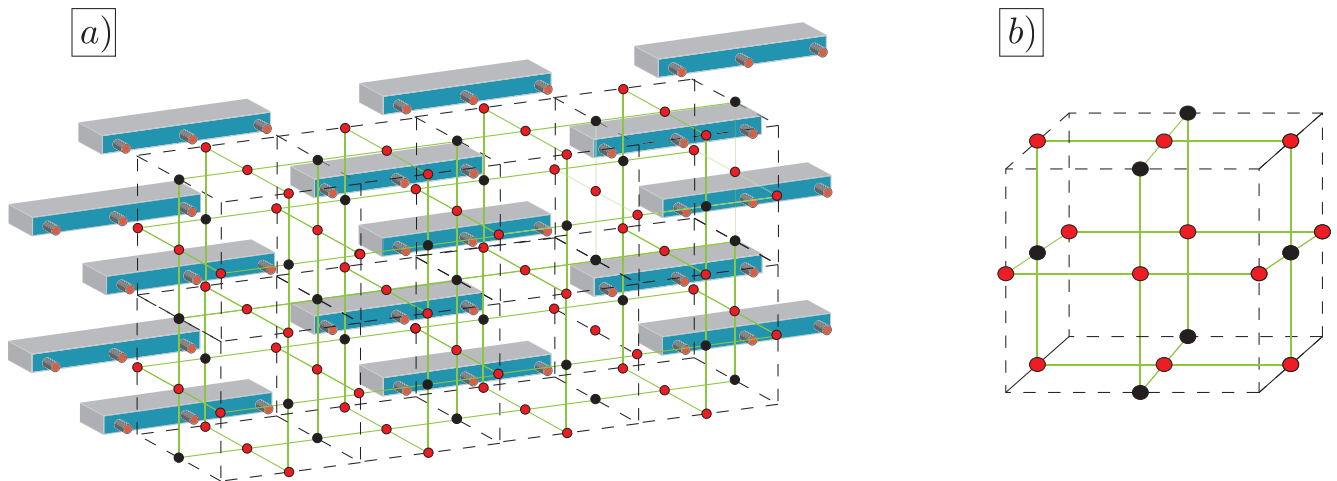


FIG. 2: **a). General layout of the optical architecture. b) Unit cell of the three dimensional lattice required to implement topological cluster state computation.** Illustrated in Fig. a. is a partial schematic of a large scale topological cluster computer. Layers of photonic chips are utilized to prepare the entanglement links between photons. Shown here is only one of the four stages of the preparation network for clarity. Photons enter the network from the rear and exit the front linked up in the required cluster state. Single photon detectors can then be placed immediately after the preparation network to consume the cluster, performing computation. This eliminates the need for photon routing and storage as each individual photon essentially follows a linear trajectory from the source, through the photonic chip preparation network and into detectors. Fig. b. details the structure of each unit cell of the cluster. This cluster is *not* a fully connected 3D lattice, the green crosses, which represent the entanglement links, ensures that each photon is connected to four neighbors, not six. As the lattice is not fully connected, there are two groups of optical lines, one set runs at a fixed repetition rate (the red photons shown above) and the other operates at half that rate (black photons) which we denote as full and half rate lines respectively.

these projections and prepare the 3D lattice. The photonic module, which lies at the heart of each chip, is designed to project an arbitrary N photon state into a ± 1 eigenstate of the operator $X^{\otimes N}$ [32], where N is the number of photons sent through the module between initialization and measurement of the atomic system. In order to perform a parity check of the operator $ZZXZZ$, Hadamard plates are placed on every input and output port, changing the projector from $X^{\otimes N}$ to $Z^{\otimes N}$. For every group of five photons sent through between initialization and measurement, the central photon in the stabilizer operator will be routed through a second set of Hadamard plates before and after passing through the module converting the projector from $ZZZZZ$ to $ZZXZZ$.

In total there are four stages required to prepare the 3D lattice. The four stages are partitioned into two groups which have identical layout and switching pattern. These two groups stabilize the lattice with respect to the side stabilizer operators and the top/bottom stabilizer operators respectively. If an arbitrary input state was utilized to prepare the cluster, two additional stages would be required to stabilize the cluster with respect to the face operators. However we can eliminate the need to perform these parity checks by carefully choosing the initial product state that is fed into the preparation network.

Each face stabilizer involves the operator $ZZXZZ$, where the operator X is centered on the photons in each half rate line (i.e. the black photons in Fig. 2). Therefore, we initially prepare each photon in the half rate optical lines in the state $|+\rangle = (|H\rangle + |V\rangle)/\sqrt{2}$ (a $+1$ eigenstate of X) while the photons in the full rate optical lines are initialized in the state $|H\rangle$ (a $+1$ eigenstate of Z). This initialization ensures that the stabilizer set for the initial state is X_i , $i \in h$ and Z_j , $j \in f$, where h and f are the sets containing photons in the half and full rate optical lines respectively. As any product of stabilizers is also a stabilizer of the system, each of the face stabilizers of the cluster are automatically satisfied. It can be easily checked that by measuring the stabilizers along the sides and the top and bottom of each unit cell removes all the operators in the original stabilizer set *except* for the $ZZXZZ$ term associated with each face stabilizer. Therefore, by the intelligent initialization of the system, the total size of the preparation network is reduced by a third, a significant optimization in the preparation of the required cluster.

Fig 3 illustrates a 2D cross section of the preparation network. We illustrate only two stages of the network since the preparation for the side stabilizers is identical to the top/bottom stabilizers. Each stage requires a staggered arrangement of photonic chips and in Fig 3, after a specific stage, we have detailed the stabilizer that has been measured where the central photon corresponds to the X operator in the measured operator. The temporal staggering of the photonic state, for each optical line, is also detailed where the spacing interval, T , is bounded below by the minimum interaction time required for the operation of the photonic module and bounded above by the coherence

time of the atomic systems in each chip.

Before detailing the switching sequence for these stages we have to address a slight complication that arises when creating the 3D lattice. In general, each photon is involved in five separate parity checks (one for each stabilizer operator involving a given qubit). As noted previously, by utilizing a specific input state we can remove the need to measure the stabilizers associated with the faces of each unit cell. This implies that we are measuring four operators for each photon present in a half rate optical line (we no longer perform a parity check associated with the face stabilizer for these photons) and three operators for each photon in a full rate optical line (each of these photons are involved in two parity checks associated with face stabilizers). As each photon suffers a temporal delay of T by passing through a photonic module, there is a temporal discrepancy with the half rate and full rate optical photons which, if not compensated, leads to two photons being temporally synchronous in a later parity check in the network. However we can use the flexibility of the photonic chips to solve the delay problem in a convenient way.

If a delay was not required, a given module has a window of $3T$ where it is idle between parity checks. Normally we would utilize this window to perform measurement and re-initialization of the atomic system. For a given stage of the preparation network, every fourth photon in a full rate optical line is not involved in any parity check and must be delayed, hence this $3T$ window is partitioned into three steps. Immediately after the last photon from the previous parity check exits the chip, the atomic system is measured (now utilizing a temporal window of T rather than $3T$). As the delayed photon is the next one to enter the chip, we simply do not initialise the module in to the required atomic superposition state. As detailed in [33], the atom/photon interaction required for the module requires initializing a 3-level atomic system into the state $(|1\rangle + |2\rangle)/\sqrt{2}$ with a resonant RF field. The presence of a photon in the cavity mode (which is detuned with the $|1\rangle \leftrightarrow |3\rangle$ transition) induces a phase shift on the state $|1\rangle$ which oscillates the system between the states $(\pm|1\rangle + |2\rangle)/\sqrt{2}$. If we instead keep the atomic system in the $|1\rangle$ (or $|2\rangle$) state, the presence of a photon will have no effect on the atomic system. Therefore, delaying the required photon by T requires operating the module as usual, but for this first step we do not initialize the atomic system. This stage again takes time T and we refer to it as a ‘‘holding’’ stage.

Finally, in the next time step we re-initialize the atomic system in the appropriate superposition state and allow the next group of five photons to proceed as normal. This trick will maintain the temporal staggering of the photons without the need for additional technology and ensures that every photonic chip is active for all time steps (no idle time for any module). Please note that technically we do not need to perform this trick in stages one or four of the preparation, as the photons from the source can be temporally staggered to account for this required delay in stage one and are measured out as part of the computation immediately after stage four. However, Fig. 3 assumes the delay is employed for conceptual simplicity.

As mentioned, there is one disadvantage to this solution. The switching sequence with no delay allows for a $3T$ window between parity checks performed using the same photonic chip. This window can be utilized for measurement and re-initialization of the atomic system. Utilizing the module to delay a photon, by holding the atomic system, reduces both the measurement and re-initialization windows to T . This has minor implications for optimization as this disadvantage could be eliminated by delaying the required photon in a dedicated unit (rather than using a photonic chip). However, since utilizing the chip to delay photons does not require any changes to the underlying design of the unit, and the temporal cost is marginal, in the short term this may be an acceptable penalty for a reduction in the overall complexity of the architecture.

Fig. 3 and Tab. I only illustrate the network and switching sequence for the stabilizers associated with the sides of the unit cell. The stabilizers associated with the top and bottom of each unit cell are measured using precisely the same network and switching sequence (when viewing the lattice from above or below). The only difference in the switching sequence has an offset of $2T$ to account for the delay from stages one and two.

By examining Fig. 3 there is the potential for photon collisions for chip layers two and four. However, whenever two photons enter a chip simultaneously, one interacts with the module while the other is required to bypass the unit. Hence the notation used in Tab. I, $\{.\}^{U,B}$ refers to switching the central port $\{.\}$ to the module while switching the photon in the (U)pper or (B)ottom port to a bypass line.

I. RESOURCE REQUIREMENTS.

While we have only illustrated the network for a 5×5 continuously generated lattice, the patterning of photonic chips and the switching sequence for each unit extends in two-dimensions allowing for the continuous generation of an arbitrary large 3D lattice. The total number of photonic chips required for the preparation of a large cross section of the lattice is easily estimated. In general, for an $N \times N$ cross section of cells, $4N^2 + 4N$ photonic chips are required to continually generate the lattice.

When high fidelity single photon sources and detectors are available, we are able to choose the optimal running time of the computer, T , as the fundamental atom/photon interaction time within each photonic module. As shown

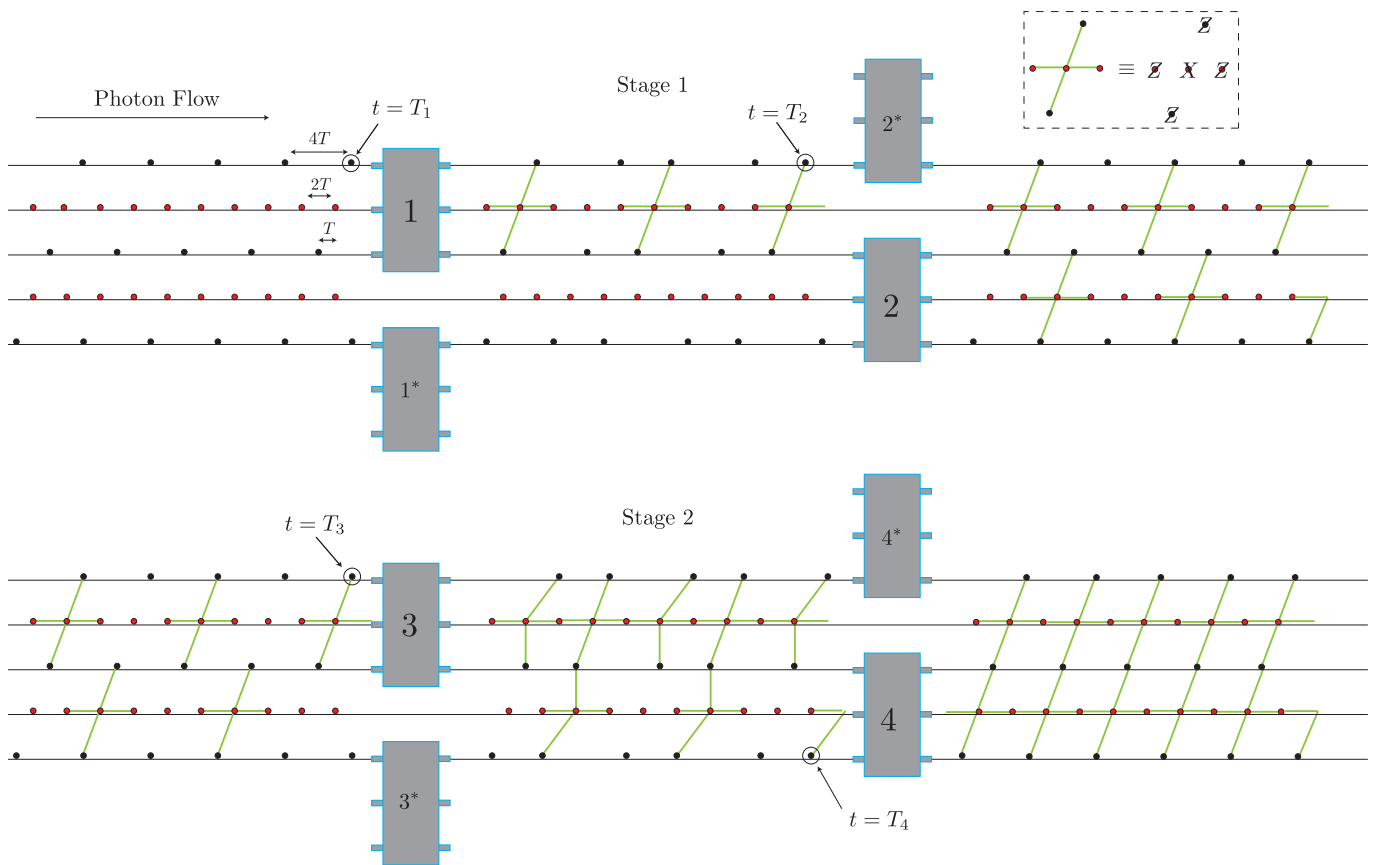


FIG. 3: **Chip orientation for stages one and two of the preparation network, utilized to measure the stabilizer operators for the sides of each unit cell.** Photons flow from left to right through each chip. The temporal staggering of each photon is required such that only one photon passes through each photonic module at any given time step. The fundamental temporal staggering is the atom/photon interaction time T , however each row has to be temporally offset to ensure proper temporal ordering for future stages. Each stage measures a specific stabilizer, illustrated with a cross after the specific stage. The operator that is measured is $ZZXZZ$, where the X operator associated with the photon at the center of the cross (insert). Extending this network to more and more cells require extending each column vertically. The network for stages three and four, required to stabilize the system with respect to the top and bottom operators of the lattice, is identical. In this case, the perspective would be looking at the cell from the top of the lattice and the switching sequence is offset by $2T$.

in Tab. I, the switching sequence for the preparation network allows for a temporal window of T for the measurement of the atomic system within each device. As estimated in [32], depending on the system used, this rate can be approximately 10ns to $1\mu\text{s}$. If we choose T to be the optimal operating rate of the photonic module, then there is the potential that atomic measurement in the preparation network is too slow. This can be overcome by the availability of more photonic chips. If more chips are available then we can construct multiple copies of the preparation network with optical switches placed between columns of photonic chips. While the atomic systems are being measured from one round of parity checks the next set of incoming photons are switched to a different group of chips.

For a given ratio of the atom/photon interaction time to atomic measurement time, $T_{\text{atom}}/T_{\text{module}} \geq 1$ (assuming that atomic measurement is always slower than the atom/photon interaction time), photons will be routed to multiple copies of the perpetual network. Therefore the number of additional photonic modules/chips will increase by a factor of $\Gamma = O(T_{\text{atom}}/T_{\text{module}})$ to compensate for slow measurement. Resource estimates are consequently related to the total 2D cross section of the lattice and Γ .

Given that the number of photonic chips required in the preparation network, for a continuously generated $N \times N$ cross section of unit cells, is $4N^2 + 4N$ (assuming $\Gamma = 1$). The number of fabricated photonic chips required when atomic measurement is slow will be approximately $\Gamma(4N^2 + 4N)$.

To put these resource costs in context we can make a quick estimate of the resources required to build a quantum computer capable of solving interesting problems. Let us choose a logical error rate per time step of 10^{-16} to be our target error rate, where a time step is the creation and measurement of a single cell. This error rate would be sufficiently low to enable the factoring of integers several thousand binary digits long using Shor's algorithm [37]. Let

Chip	1	2	3	4	5	6	7	8	9	10	11	12	13
1	U	C	B	L	M	H	I	R	U	C	B	L	M
1*	M	H	I	R	U	C	B	L	M	H	I	R	U
2	B	L	M	H^U	I	R^B	U	C	B	L	M	H^U	I
2*	I	R^B	U	C	B	L	M	H^U	I	R^B	U	C	B
3	B	L	M	H	I	R	U	C	B	L	M	S	I
3*	I	R	U	C	B	L	M	H	I	L	U	C	B
4	M	H^U	I	R^B	U	C	B	L	M	H^U	I	R^B	U
4*	U	C	B	L	M	H^U	I	R^B	U	C	B	L	M

TABLE I: Switching sequence for stages one and two of the photonic chip network where this 2D cross section represents the side of the unit cell. We have not illustrated stages three and four as the spatial arrangement of chips and the switching sequences are identical when examining a cross section the cluster from above (the switching sequence for stages three and four will have a $2T$ offset from the one shown above). The temporal location of each of the photons at $t = \{T_1, T_2, T_3, T_4\}$ is indicated in Fig. 3. The labels R, L, C, U, B refer to the geometric arrangement of the photons in the lattice stabilizer (i.e. right, left, center, upper and bottom) while the switching settings are $R = C = L =$ central chip port, $U =$ upper chip port $B =$ lower chip port, $M =$ Measure the atomic system $I =$ Initialize the atomic system in the $(|1\rangle + |2\rangle)/\sqrt{2}$ state and H indicating to “hold” the atomic system in the $|1\rangle$ state in order to delay a photon not involved in any stabilizer check by T . In chip layers two and four, temporally synchronous photons enter a particular chip, however only one of these photons is routed into the module. These stages are indicated by $\{.\}^{U,B}$, denoting the port (either U or B) that is routed through the bypass in that time step. Additionally, for a given column of chips, there are two switching sequences, (one denoted by $*$) which repeats down any given column.

us assume that increasing the separation between defects and the circumference of defects by two cells reduces the logical error rate per time step by a factor of 100. Given the threshold error rate of the 3-D topological cluster state scheme is 6.7×10^{-3} [38], albeit in the absence of loss, this assumption is equivalent to assuming qubits are affected by Z errors with a probability between 10^{-4} and 10^{-5} per time step.

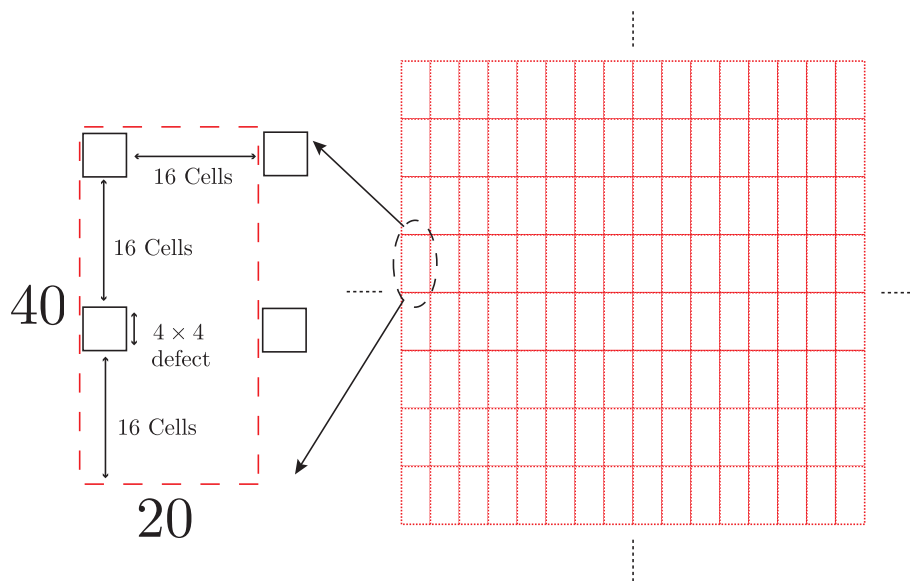


FIG. 4: **Large scale lattice structure required for long term computation via topological cluster states.** Here we illustrate a basic concept of the lattice structure that is required for lengthy operations of the topological optical computer (when examining the lattice from the front). Based on the estimates in the main text, each logical qubit (defined via a pair of defects in the lattice) requires a 40×20 array of cells. The layout for each logical qubit is shown on the left, with the larger lattice, comprising thousands (if not millions) of logical qubits shown on the right. Each logical qubit requires just over 3000 fabricated photonic chips. As a quick estimate, the topological error protection afforded by this sized lattice allows for a computation requiring approximately 10^{16} logical operations.

Given the above assumptions, the desired logical error rate per time step could be achieved with defects measuring 4×4 cells in cross-section and separated by 16 cells. Fig. 4 shows a section of a semi-infinite lattice of sufficiently well

error corrected logical qubits. Each logical qubit occupies a region of 40×20 cells. To prepare such a lattice (for an arbitrary number of time steps and setting $\Gamma = 1$ for convenience) we would require the fabrication of 3320 integrated photonic chips.

Even with this basic estimate, the resource requirements of this architecture are promising. The high fidelity construction of approximately 3×10^3 photonic modules, per logical qubit, to prepare a lattice that has sufficient topological protection to perform on the order of 10^{16} logical gate operations is arguably a less significant challenge than the high fidelity manufacturing of other proposed quantum computer architectures. Other proposed systems not only require comparable (if not more) physical qubits to achieve the same error protection, but depending on the system they will require interconnected quantum bus systems for qubit transport, very non-trivial classical control structures and most likely the fabrication of the entire computer at once, with little flexibility to expand the size of the computer as more resources become available.

II. CONCLUSIONS

We have presented a detailed architecture for topological cluster state computation utilizing the photonic module and photonic chip as the primary operational elements. This design solves many of the significant hurdles limiting the practical scalability of optical quantum computation, namely the inherent engineering problems associated with probabilistic photon/photon interactions and the apparent intractability of designing large scale, chip based systems which can be scaled to millions of qubits.

Additionally, by utilizing topological cluster states as the underlying computational model we achieve an architecture exhibiting high thresholds which incorporates photon loss (which is problematic in traditional 2D cluster state computing) into an error channel correctable without additional codes or technologies.

The experimental feasibility of constructing this type of computer is promising. High fidelity coupling of single photons to colour centers in cavities is a significant area of research in the quantum computing community and the nano engineering required to produce a high fidelity photonic module is arguably much simpler than a full scale atom/cavity based quantum computer which would require the fabrication of all data qubits and interconnected transport buses simultaneously. An additional benefit is the continuous nature of the lattice preparation. The required number of photonic modules and photonic chips only depends on the 2D cross sectional size of the lattice. Therefore, once an appropriate number of devices are available to prepare a given number of cells, the number of computational times steps is arbitrary, highlighting the advantages of having photons as disposable quantum computational resources.

As well as presenting the preparation network constructed from photonic chips there is the additional possibility of constructing the entire architecture completely using photonic modules. This current architecture design assumes the availability of high fidelity single photon sources and detectors. However, it is well known that the parity gate afforded by the photonic module is also sufficient to act as sources and detectors [39]. Consequently the entire computer architecture can conceivably be built using no other quantum information devices except for the photonic module and photonic chip, reducing again the technological barrier of engineering several different high fidelity quantum components for a large scale computer.

III. ACKNOWLEDGMENTS

The authors thank C.-H. Su for helpful discussions. The authors acknowledge the support of MEXT, JST, the EU project QAP, the Australian Research Council, the Australian Government, the US National Security Agency (NSA), Army Research Office (ARO) under Contracts Nos. W911NF-05-1-0284.

-
- [1] R. Raussendorf and J. Harrington, *Phys. Rev. Lett.* **98**, 190504 (2007).
 - [2] R. Raussendorf, J. Harrington and K. Goyal, *New J. Phys.* **9**, 199 (2007).
 - [3] A.G. Fowler, A.M. Stephens and P. Groszkowski, *arXiv:0803.0272* (2008).
 - [4] A.G. Fowler and K. Goyal, *arXiv:0805.3202* (2008).
 - [5] R. Raussendorf, H.J. Briegel, *Phys. Rev. Lett.* **86**, 5188 (2001).
 - [6] C. Nayak, S.H. Simon, A. Stern, M. Freedman and S. Das Sarma, *arXiv:0707.1889* (2007).
 - [7] Y. Nakamura, Yu. A. Pashkin and J.S. Tsai. *Nature (London)* **398**, 786 (1999).
 - [8] I. Chiorescu, Y. Nakamura, C.J.P.M. Harmans and J.E. Mooij, *Science* **299**, 1869 (2003).
 - [9] T. Yamamoto, Yu. A. Pashkin, O. Astafiev, Y. Nakamura and J.S. Tsai *Nature (London)* **425**, 941 (2003).

- [10] J. Chiaverini, D. Leibfried, T. Schaetz, M.D. Barrett, R.B. Blakestad, J. Britton, W.M. Itano, J.D. Jost, E. Knill, C. Langer, R. Ozeri and D.J. Wineland. *Nature (London)* **432**, 602 (2004).
- [11] H. Häffner, W. Hänsel, C.F. Roos, J. Benhelm, D. Chek-al-kar, M. Chwalla, T. Körber, U.D. Rapol, M. Riebe, P.O. Schmidt, C. Becher, O. Gühne, W. Dür and R. Blatt. *Nature (London)* **438**, 643 (2005).
- [12] J. Gorman, D.G. Hasko and D.A. Williams. *Phys. Rev. A* **95**, 090502 (2005).
- [13] T. Gaebel, M. Domhan, I. Popa, C. Wittmann, P. Neumann, F. Jelezko, J.R. Rabeau, N. Stavrias, A.D. Greentree, S. Prawer, J. Meijer, J. Twamley, P.R. Hemmer and J. Wrachtrup. *Nature (Physics)* **2**, 408 (2006).
- [14] R. Hanson, F.M. Mendoza, R.J. Epstein, and D.D. Awschalom. *Phys. Rev. Lett.* **97**, 087601 (2006).
- [15] M.V. Gurudev Dutt, L. Childress, L. Jiang, E. Togan, J. Maze, F. Jelezko, A.S. Zibrov, P.R. Hemmer, and M.D. Lukin. *Science* **316**, 1312 (2007).
- [16] J.L. O'Brien, G.J. Pryde, A.G. White, T.C. Ralph, and D. Branning. *Nature (London)* **426**, 264 (2003).
- [17] E. Knill, R. Laflamme, and G. Milburn, *Nature* **409**, 46 (2001).
- [18] P. Kok, W.J. Munro, K. Nemoto, T.C. Ralph, J.P. Dowling, and G.J. Milburn. *Rev. Mod. Phys.* **79**, 135 (2007).
- [19] M.A. Nielsen, *Phys. Rev. A* **93**, 040503 (2004).
- [20] C.M. Dawson, H.L. Haselgrove and M.A. Nielsen, *Phys. Rev. A*, **73**, 052306 (2006).
- [21] T.C. Ralph, A.J.F. Hayes and A. Gilchrist, *Phys. Rev. Lett.* **95**, 100501 (2005).
- [22] M. Varnava, D.E. Browne and T. Rudolph, *Phys. Rev. Lett.*, **100**, 160502 (2008).
- [23] M.A. Nielsen and C.M. Dawson, *Phys. Rev. A* **71**, 042323 (2005).
- [24] K.M. Svore, D.P. DiVincenzo, and B.M. Terhal. *Quant. Inf. Comp.* **7**, 297 (2007).
- [25] A.M. Stephens, A.G. Fowler, and L.C.L. Hollenberg. *Quant. Inf. Comp.* **8**, 330 (2008).
- [26] P. Aliferis, D. Gottesman, and J. Preskill. *Quant. Inf. Comp.* **6**, 97 (2006).
- [27] C.W.J. Beenakker, D.P. DiVincenzo, C. Emary, and M. Kindermann, *Phys. Rev. Lett.* **93**, 020501 (2004);
- [28] K. Nemoto and W.J. Munro, *Phys. Rev. Lett.* **93**, 250502 (2004).
- [29] P. Domokos, J.M. Raimond, M. Brune and S. Haroche. *Phys. Rev. A* **52**, 3554 (1995).
- [30] L.-M. Dun and H.J. Kimble. *Phys. Rev. Lett.* **92**, 127902 (2004).
- [31] T.P. Spiller, K. Nemoto, S.L. Braunstein, W.J. Munro, P. van Loock, G.J. Milburn, *New J. Phys.* **8**, 30 (2006).
- [32] S.J. Devitt, A.D. Greentree, R. Ionicioiu, J.L. O'Brien, W.J. Munro and L.C.L. Hollenberg *Phys. Rev. A* **76**, 052312 (2007).
- [33] A.M. Stephens, Z.W.E. Evans, S.J. Devitt, A.G. Fowler, A.D. Greentree, W.J. Munro, J.L. O'Brien, K. Nemoto and L.C.L. Hollenberg, *arXiv:0805.3592*, (2008).
- [34] E. Knill, *Nature (London)* **434**, 39 (2005).
- [35] K. Kieling, T. Rudolph, and J. Eisert. *Phys. Rev. Lett.* **99**, 130501 (2007).
- [36] D. Gottesman, Ph.D Thesis (Caltech), *quant-ph/9705052*, (1997).
- [37] P.W. Shor, *SIAM J. of Computing*, **26**, 1484 (1997).
- [38] R. Raussendorf, J. Harrington and K. Goyal, *Ann. Phys.* **321**, 2242 (2006).
- [39] K. Nemoto and W.J. Munro, *Phys. Lett. A* **344**, 104 (2005).